INVESTIGATIONS OF QCD HADRONIZATION USING JETS MEASURED AT $\sqrt{s} = 8$ TeV WITH THE ALICE DETECTOR.

A Dissertation Presented for the
Doctor of Philosophy
Degree
The University of Tennessee, Knoxville

Andrew John Castro

March 2019

Table of Contents

List of Figures

Chapter 1

Jet Results and Discussion

Beginning in March of 2012, the LHC began seven months of pp collisions at $\sqrt{s} =$ 8 TeV. The jet cross sections and ratios of the cross sections for jets of different radii offers a unique perspective on the pQCD effects of hadronization at this new energy frontier. Due to the expectation that no QGP is formed in a pp collision these measurements serve as a baseline for separating phenomena associated with the QGP in heavy-ion collisions. In order to measure the jet cross section the following formula is used,

$$\frac{d\sigma^{jet}}{d\eta\, dp_T} = \frac{A_{trigger}}{\epsilon_{trigger}(p_T)} \times C_{MC} \times \frac{1}{A(p_T)} \times \frac{1}{\mathscr{L}_{int}} \times \frac{dN^{jet}}{dp_T\, d\eta} \tag{1.1}$$

where,

- $A_{trigger}$ is the acceptance for EMCal triggered events and $\epsilon_{trigger}(p_T)$ is the EMCal trigger efficiency. These factors correct for imperfections in the electronics of the EMCal and the overall factors are equal to one in minnimum bias events.
- C_{MC} is a correction factor due to detector effects and it allows for comparisons between the ALICE experiment to other experiments or theoretical calculations. Unfolding is used to determine this factor.
- L_{int} is the integrated luminosity during the period when the data was recorded.
- $A(p_T)$ is the geometrical detector acceptance.

- $\frac{dN^{jet}}{dp_T\, d\eta}$ is the inclusive jet momentum spectra.

The following sections will go over how each factor was determined and the quality assurance procedures used for this analysis.

1.1 Data Quality

ALICE is a state-of-the-art experiment with excellent tracking and particle identification capabilities as discussed in Chapter ??. However, just like any real world experiment, it contains a number of inefficiencies and imperfections. This means that the data collected during the 8 TeV pp collision must be examined and any inaccuracies in the data must be removed before hard physics conclusions may be reached. Data may be compromised at both the event-level, the experiment erroneously recorded something as an event, or at the constituent-level, one of the subdetectors mismeasured a feature of a particle, and these outliers must be accounted for and removed

1.2 Event Selection

For an event to be selected into a physics analysis it must pass a number of quality control tests. For example, the LHC must have be in a state of stable beams, cosmic rays must be excluded by only accepting tracks that originate from a vertex inside the detector, and the relevant detectors for a given analysis must be functioning as intended.

During the 8 TeV data collection period approximately 180 million minimum bias events were recorded, as summarized in table ??. These events are separated into periods, which dictate the particular beam and detector configurations during the data taking.The 8 TeV data is broken into 7 periods with approximately 181 million minimum bias events recorded.

Approximately, 15% of the data sampled is unusable due to malfunctions in TPC chambers, EMCal super modules, the electronics for the EMCal or TPC, and

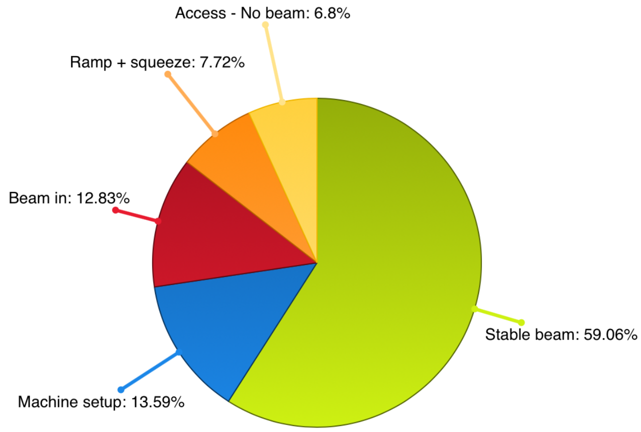

Figure 1.1: LHC state during the 8 TeV run.

1.3 Raw measurements

The ALICE experiment is capable of two types of jet reconstruction, charged and full jets. Charged jets use information from the charged particle tracking detectors, such as the ITS and TPC, in conjunction with a jet finding algorithm to identify jets. Full jets implement a similar procedure but also incorporates the EMCal in order to

Period	# of runs	# of Min Bias events
LHC12c	89	$\sim$24 M
LHC12d	140	$\sim$62 M
LHC12e	5	$\sim$2 M
LHC12f	56	$\sim$15 M
LHC12g	8	$\sim$0.4 M
LHC12h	159	$\sim$75 M
LHC12i	40	$\sim$3 M
Total	497	$\sim$181 M

Table 1.1: 2012 8 TeV data taking period.

1.3.1 Raw Jet Momentum Spectra in pp Collisions

1.4 Unfolding

1.4.1 Corrections to particle Level

1.4.2 Unfolding Matrix

1.4.3 Unfolded Spectra

1.5 EMCal Triggered Data

In addition with the minimum bias data collected, the EMCal was used during the 8 TeV run in order to provided an enhanced data set that is preferential to hard processes. The Level-1 trigger[**?**] in the EMCal

$$Trigger\,Efficency = \frac{N_{events}^{Triggered}}{N_{events}^{MinBias}} \times \frac{d^2 N_{Triggered}^{jet}}{d\eta\, dp_T} \bigg/ \frac{d^2 N_{MinBias}^{jet}}{d\eta\, dp_T} \tag{1.2}$$

1.6 Systematic Uncertainties

1.6.1 Systematic Uncertainty to Jet Yield

1.6.2 Systematic Uncertainty to Jet Energy Scale

Luminosity Uncertainty

The luminosity of a hadronic collider, $\mathscr{L}$, is given by the expression

$$\mathscr{L} = \frac{R}{\sigma} \tag{1.3}$$

The luminosity along with its uncertainity were determined during a a special Van der Meer scan run in April of 2012[**?**].

1.6.3 Total Uncertainty

1.7 Corrected pp jet cross section

1.7.1 Comparisons to pQCD predictions

1.7.2 Jet Cross Section and Ratios

Given two jets of different radii, R_1 and R_2, the ratio of the cross sections may be written in short hand as,

$$\frac{\sigma_{R_1}}{\sigma_{R_2}} = \frac{d\sigma^{jet}_{R_1}}{dp_T} \Bigg/ \frac{d\sigma^{jet}_{R_2}}{dp_T} \tag{1.4}$$

Chapter 2

Conclusion and Outlook

Bibliography

[1] C. Patrignani et al. Review of Particle Physics. *Chin. Phys.*, C40(10):100001, 2016. v, 15

[2] Vardan Khachatryan et al. Measurement of the inclusive 3-jet production differential cross section in proton–proton collisions at 7 TeV and determination of the strong coupling constant in the TeV range. *Eur. Phys. J.*, C75(5):186, 2015.

[3] Esma Mobs. The CERN accelerator complex. Complexe des accélérateurs du CERN. Jul 2016. General Photo.

[4] W. M. Alberico, A. Beraudo, A. De Pace, A. Molinari, M. Monteno, M. Nardi, and F. Prino. Heavy-flavour spectra in high energy nucleus-nucleus collisions. *Eur. Phys. J.*, C71:1666, 2011.

[5] Jaroslav Adam et al. Centrality dependence of the charged-particle multiplicity density at midrapidity in Pb-Pb collisions at $\sqrt{s_{\rm NN}} = 5.02$ TeV. *Phys. Rev. Lett.*, 116(22):222302, 2016.

[6] J. Alme et al. The ALICE TPC, a large 3-dimensional tracking device with fast readout for ultra-high multiplicity events. *Nuclear Instruments and Methods in Physics Research A*, 622:316–367, October 2010.

[7] Ralf Diener. Gas amplification with micro pattern gas detectors.

[8] Betty Bezverkhny Abelev et al. Performance of the ALICE Experiment at the CERN LHC. *Int. J. Mod. Phys.*, A29:1430044, 2014.

[9] G Bourdaud. Gamma-jet physics with the electro-magnetic calorimeter in the alice experiment at lhc. *Journal of Physics: Conference Series*, 110(3):032006, 2008.

[10] U. Abeysekara et al. ALICE EMCal Physics Performance Report. 2010.

[11] Cristiane Jahnke. J/ψ production as a function of event multiplicity in pp collisions at $\sqrt{s} = 13$ TeV using EMCal-triggered events with ALICE at the LHC. In *14th International Workshop on Hadron Physics (Hadron Physics 2018) Florianopolis, Santa Catarina, Brazil, March 18-23, 2018*, 2018.

[12] B Abelev et al. Upgrade of the ALICE Experiment: Letter of Intent. Technical Report CERN-LHCC-2012-012. LHCC-I-022. ALICE-UG-002, CERN, Geneva, Aug 2012.

[13] Erik Brücken and Timo Hildén. GEM Foil Quality Assurance For The ALICE TPC Upgrade. *EPJ Web Conf.*, 174:03004, 2018.

[14] Purba Bhattacharya, Bedangadas Mohanty, Supratik Mukhopadhyay, Nayana Majumdar, and Hugo Natal da Luz. 3D simulation of electron and ion transmission of GEM-based detectors. *Nucl. Instrum. Meth.*, A870:64–72, 2017.

[15] Dick Majka. The alice tpc upgrade project. Quark Matter 2017, 2017.

[16] Upgrade of the ALICE Time Projection Chamber. Technical Report CERN-LHCC-2013-020. ALICE-TDR-016, Oct 2013.

[17] Addendum to the Technical Design Report for the Upgrade of the ALICE Time Projection Chamber. Technical Report CERN-LHCC-2015-002. ALICE-TDR-016-ADD-1, Feb 2015.

[18] Jens Erik Brücken and Timo Eero Hildén. The GEM QA Protocol of the ALICE TPC Upgrade Project. In *5th International Conference on Micro Pattern Gas Detectors (MPGD2017) Temple University, Philadelphia, USA, May 22-26, 2017*, 2018.

[19] Francesco Noferini. The ALICE PID performance in Run 1 and perspectives in view of Run 2. In *Proceedings, 3rd Large Hadron Collider Physics Conference (LHCP 2015): St. Petersburg, Russia, August 31-September 5, 2015*, pages 523–528, Gatchina, 2016. Kurchatov Institute, Kurchatov Institute. v, 16

[20] Paul Langacker. Introduction to the Standard Model and Electroweak Physics. In *Proceedings of Theoretical Advanced Study Institute in Elementary Particle Physics on The dawn of the LHC era (TASI 2008): Boulder, USA, June 2-27, 2008*, pages 3–48, 2010.

[21] Tatsumi Aoyama, M. Hayakawa, Toichiro Kinoshita, and Makiko Nio. Tenth-Order Electron Anomalous Magnetic Moment — Contribution of Diagrams without

Closed Lepton Loops. *Phys. Rev.*, D91(3):033006, 2015. [Erratum: Phys. Rev.D96,no.1,019901(2017)].

[22] Michael Riordan. The discovery of quarks. *Science*, 256(5061):1287–1293, 1992.

[23] Frank Wilczek. Asymptotic freedom: From paradox to paradigm. *Proc. Nat. Acad. Sci.*, 102:8403–8413, 2005. [Rev. Mod. Phys.77,857(2005)].

[24] Constantin Loizides. Glauber modeling of high-energy nuclear collisions at the subnucleon level. *Phys. Rev.*, C94(2):024914, 2016.

[25] Michael L. Miller, Klaus Reygers, Stephen J. Sanders, and Peter Steinberg. Glauber modeling in high energy nuclear collisions. *Ann. Rev. Nucl. Part. Sci.*, 57:205–243, 2007.

[26] J E Huth, N Wainer, K Meier, N J Hadley, F Aversa, Mario Greco, P Chiappetta, J P Guillet, S Ellis, Zoltán Kunszt, and Davison Eugene Soper. Toward a standardization of jet definitions. (FERMILAB-CONF-90-249-E):7 p, Dec 1990.

[27] STEPHEN MYERS. The large hadron collider 2008–2013. *International Journal of Modern Physics A*, 28(25):1330035, 2013.

[28] Thomas Taylor and Daniel Treille. The Large Electron Positron Collider (LEP): Probing the Standard Model. *Adv. Ser. Direct. High Energy Phys.*, 27:217–261, 2017.

[29] G. Aad et al. The ATLAS Experiment at the CERN Large Hadron Collider. *JINST*, 3:S08003, 2008.

[30] S. Chatrchyan et al. The CMS Experiment at the CERN LHC. *JINST*, 3:S08004, 2008.

[31] A. Augusto Alves, Jr. et al. The LHCb Detector at the LHC. *JINST*, 3:S08005, 2008.

[32] K. Aamodt et al. The ALICE experiment at the CERN LHC. *JINST*, 3:S08002, 2008.

[33] Serguei Chatrchyan et al. Observation of a new boson at a mass of 125 GeV with the CMS experiment at the LHC. *Phys. Lett.*, B716:30–61, 2012.

[34] Georges Aad et al. Observation of a new particle in the search for the Standard Model Higgs boson with the ATLAS detector at the LHC. *Phys. Lett.*, B716:1–29, 2012.

[35] C. Fabjan and J. Schukraft. The Story of ALICE: Building the dedicated heavy ion detector at LHC. In *'The Large Hadron Collider: A marvel technology', EPFL-Press Lausanne, Switzerland, 2009 (Editor: L. Evans), chapter 5.4*, 2011.

[36] Vladimir V. Gligorov, Simon Knapen, Benjamin Nachman, Michele Papucci, and Dean J. Robinson. Leveraging the ALICE/L3 cavern for long-lived exotics. 2018.

[37] M. Bondila et al. ALICE T0 detector. *IEEE Trans. Nucl. Sci.*, 52:1705–1711, 2005.

[38] E. Abbas et al. Performance of the ALICE VZERO system. *JINST*, 8:P10016, 2013.

[39] Rick Field. Min-Bias and the Underlying Event at the LHC. *Acta Phys. Polon.*, B42:2631–2656, 2011.

[40] S. Beolè. The alice inner tracking system: Performance with proton and lead beams. *Physics Procedia*, 37:1062 – 1069, 2012. Proceedings of the 2nd International Conference on Technology and Instrumentation in Particle Physics (TIPP 2011).

[41] Jaroslav Adam et al. Particle identification in ALICE: a Bayesian approach. *Eur. Phys. J. Plus*, 131(5):168, 2016.

[42] Christian Lippmann. Performance of the alice time projection chamber. *Physics Procedia*, 37:434 – 441, 2012. Proceedings of the 2nd International Conference on Technology and Instrumentation in Particle Physics (TIPP 2011).

[43] A Fantoni and the ALICE collaboration. The alice electromagnetic calorimeter: Emcal. *Journal of Physics: Conference Series*, 293(1):012043, 2011.

[44] Olivier Bourrion, R Guernane, B Boyer, JL Bouly, and G Marcotte. Level-1 jet trigger hardware for the alice electromagnetic calorimeter at lhc. *Journal of Instrumentation*, 5(12):C12048, 2010.

[45] O Bourrion, N Arbor, G Conesa-Balbastre, C Furget, R Guernane, and G Marcotte. The alice emcal l1 trigger first year of operation experience. *Journal of Instrumentation*, 8(01):C01013, 2013.

[46] Jiri Kral, Terry Awes, Hans Muller, Jan Rak, and Joachim Schambach. {L0} trigger for the {EMCal} detector of the {ALICE} experiment. *Nuclear Instruments and Methods in Physics Research Section A: Accelerators, Spectrometers, Detectors and Associated Equipment*, 693:261 – 267, 2012.

[47] G Apollinari, I Béjar Alonso, O Brüning, M Lamont, and L Rossi. High-Luminosity Large Hadron Collider (HL-LHC) : Preliminary Design Report. 2015.

[48] Levente Molnar and the ALICE Collaboration. Upgrade and physics perspective of alice at the lhc. *Journal of Physics: Conference Series*, 589(1):012014, 2015.

[49] T L Karavicheva and ALICE Collaboration. The fast interaction trigger detector for the alice upgrade. *Journal of Physics: Conference Series*, 798(1):012186, 2017.

[50] B Abelev and all. Technical Design Report for the Upgrade of the ALICE Inner Tracking System. Technical Report CERN-LHCC-2013-024. ALICE-TDR-017, Nov 2013.

[51] Technical Design Report for the Muon Forward Tracker. Technical Report CERN-LHCC-2015-001. ALICE-TDR-018, Jan 2015.

[52] P Buncic, M Krzewicki, and P Vande Vyvre. Technical Design Report for the Upgrade of the Online-Offline Computing System. Technical Report CERN-LHCC-2015-006. ALICE-TDR-019, Apr 2015.

[53] Radoslaw Ryblewski and Michael Strickland. Dilepton production from the quark-gluon plasma using leading-order (3+1)D anisotropic hydrodynamics. *Acta Phys. Polon. Supp.*, 8(2):445, 2015.

[54] Mauricio Martinez and Michael Strickland. Measuring QGP thermalization time with dileptons. *Phys. Rev. Lett.*, 100:102301, 2008.

[55] F. Sauli. GEM: A new concept for electron amplification in gas detectors. *Nucl. Instrum. Meth.*, A386:531–534, 1997.

[56] Maxim Titov. Perspectives of Micro-Pattern Gaseous Detector Technologies for Future Physics Projects. In *Proceedings, CMS Workshop: Perspectives on Physics and on CMS at Very High Luminosity, HL-LHC: Alushta, Crimea, Ukraine, May 28–31, 2012*, pages 241–258, 2013.

[57] M Tang, A Q Liu, A Agarwal, and M H Habib. A single-mask substrate transfer technique for the fabrication of high-aspect-ratio micromachined structures. *Journal of Micromechanics and Microengineering*, 17(8):1575, 2007.

[58] W. You, Y. Zhou, J. Liu, M. Shao, C. Li, H. Chen, Z. Tang, Y. Sun, Y. Zhang, Y. Lv, G. Song, X. Wang, D. Hu, and D. Hong. A new technique for assembling large-size gem detectors. *Journal of Instrumentation*, 12(06):C06036, 2017.

[59] Fabio Sauli. The gas electron multiplier (gem): Operating principles and applications. *Nuclear Instruments and Methods in Physics Research Section A: Accelerators, Spectrometers, Detectors and Associated Equipment*, 805:2 – 24, 2016. Special Issue in memory of Glenn F. Knoll.

[60] Marco Santimaria and Davide Pinci. Study of the GEM detector for the LHCb experiment upgrade, Nov 2013. Presented 19 Dec 2013.

[61] S. Agostinelli et al. GEANT4: A Simulation toolkit. *Nucl. Instrum. Meth.*, A506:250–303, 2003.

[62] Betty Bezverkhny Abelev et al. Production of charged pions, kaons and protons at large transverse momenta in pp and Pb–Pb collisions at $\sqrt{s_{\mathrm{NN}}}$ =2.76 TeV. *Phys. Lett.*, B736:196–207, 2014. 16

Appendices

A Particle Identification via Bethe-Bloch

The energy loss of a relativistic charged particle traversing through a medium is given by the Bethe-Bloch relation:

$$\frac{dE}{dx} \propto \frac{1}{\beta^2}\frac{Z}{A}\rho\left[\frac{1}{2}\ln\frac{2m_ec^2\beta^2\gamma^2T_{max}}{I^2} - \beta^2 - \frac{\delta\left(\beta\gamma\right)}{2}\right] \tag{1}$$

where ρ is the density of the medium, $\frac{Z}{A}$ is the ratio of the atomic number to the atomic mass of the absorber, β is the ratio of the particle's momentum to energy, T_{max} is the maximum transfer energy from the charged particle to an electron in the medium, I^2 is the mean excitation energy of the medium, $\frac{\delta(\beta\gamma)}{2}$ is a correction factor based on the polarization of the material, and γ^2 is the lorentz factor $\frac{1}{\sqrt{1-\beta^2}}$

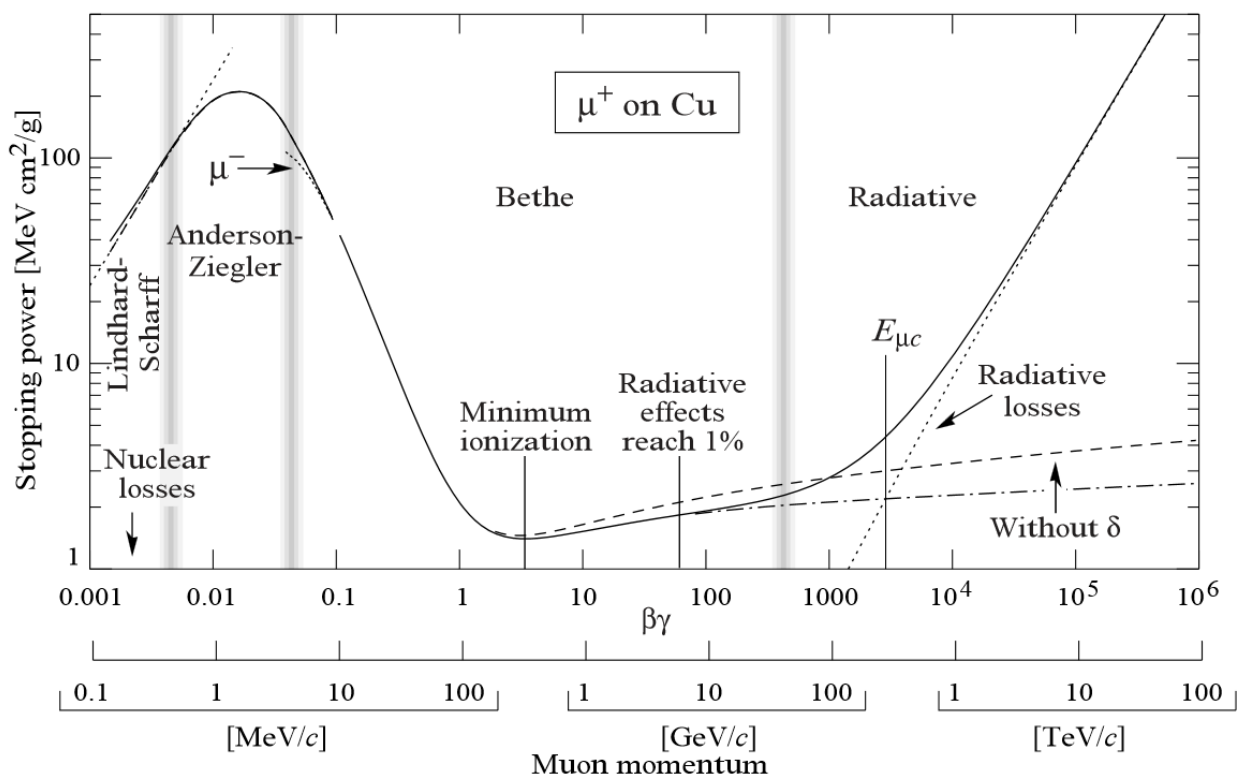

Figure 1: Energy loss of a muon traversing a copper medium between 0.1 MeV to 100 TeV [1].

Figure 1 shows the Bethe-Bloch curve for a muon over a wide kinematic range. At low energies the dominate form of energy loss is via elastic scattering, while at high energies radiation becomes the dominate energy loss mechanism. When $\beta\gamma \approx 3$ the muon losses the least amount of energy possible and is called a minimum ionization particle(MIP).

The ALICE ITS and TPC[1] cannot directly measure the energy loss of a particle traversing either sub-detector. Instead they perform PID by measuring the relative amplitudes from the sub-detectors read-out elements, pixels in the ITS and copper pads in the TPC. The amplitudes are then fit to the Bethe-Bloch equation as seen in Figure 2. Electrons weakly obey the Bethe-Bloch relationship in the kinematic ranges sensitive to the ITS and TPC and thus have a constant energy loss in both detectors.

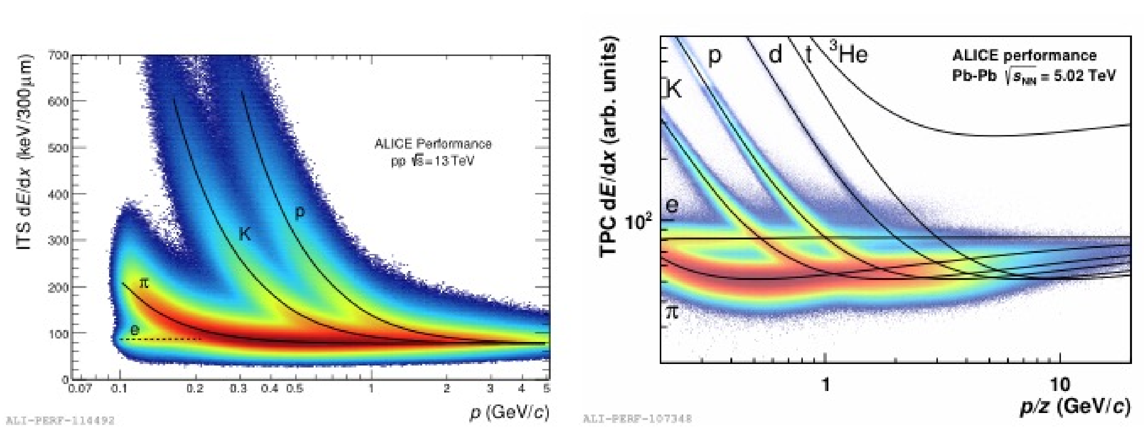

(a) ALICE ITS(pp $\sqrt{s} = 13$ TeV) **(b)** ALICE TPC (PbPb $\sqrt{s_{NN}} = 5.02$ TeV)

Figure 2: Specific energy loss for the ITS *(left)* and the TPC *(right)* with Bethe-Bloch fits from different particle species traversing each detector[19].

Figure 2 also shows that the Bethe-Bloch curves merge above some kinematic range, 4 GeV in the ITS and 10 GeV in the TPC. Above this kinematic range particles cannot be distinguished on a track-by-track basis, but by using statistical methods and Gaussian fits PID can be extended up to 20 GeV[62].

[1] See Section **??** and Section **??**

Vita